

# Anatomical Distribution of Voltage-dependent Membrane Capacitance in Frog Skeletal Muscle Fibers

CHRISTOPHER L.-H. HUANG and LEE D. PEACHEY

From the Physiological Laboratory, Cambridge CB2 3EG, United Kingdom

**ABSTRACT** Components of nonlinear capacitance, or charge movement, were localized in the membranes of frog skeletal muscle fibers by studying the effect of 'detubulation' resulting from sudden withdrawal of glycerol from a glycerol-hyper-tonic solution in which the muscles had been immersed. Linear capacitance was evaluated from the integral of the transient current elicited by imposed voltage clamp steps near the holding potential using bathing solutions that minimized tubular voltage attenuation. The dependence of linear membrane capacitance on fiber diameter in intact fibers was consistent with surface and tubular capacitances and a term attributable to the capacitance of the fiber end. A reduction in this dependence in detubulated fibers suggested that sudden glycerol withdrawal isolated between 75 and 100% of the transverse tubules from the fiber surface. Glycerol withdrawal in two stages did not cause appreciable detubulation. Such glycerol-treated but not detubulated fibers were used as controls.

Detubulation reduced delayed ( $q_\gamma$ ) charging currents to an extent not explicable simply in terms of tubular conduction delays. Nonlinear membrane capacitance measured at different voltages was expressed normalized to accessible linear fiber membrane capacitance. In control fibers it was strongly voltage dependent. Both the magnitude and steepness of the function were markedly reduced by adding tetracaine, which removed a component in agreement with earlier reports for  $q_\gamma$  charge. In contrast, detubulated fibers had nonlinear capacitances resembling those of  $q_\beta$  charge, and were not affected by adding tetracaine.

These findings are discussed in terms of a preferential localization of tetracaine-sensitive ( $q_\gamma$ ) charge in transverse tubule membrane, in contrast to a more even distribution of the tetracaine-resistant ( $q_\beta$ ) charge in both transverse tubule and surface membranes. These results suggest that  $q_\beta$  and  $q_\gamma$  are due to different molecules and that the movement of  $q_\gamma$  in the transverse tubule membrane is the voltage-sensing step in excitation-contraction coupling.

Address reprint requests to Dr. Lee D. Peachey, Department of Biology, University of Pennsylvania, Philadelphia, PA 19104-6018.

## INTRODUCTION

At least three components of voltage-dependent capacitance, which give rise to intramembrane charge movements, have been described in amphibian skeletal muscle fibers (Adrian and Peres, 1979; Huang, 1980, 1981*a*, 1982; Hui, 1983). Two of these ( $q_\beta$  and  $q_\gamma$ ) are appreciably voltage dependent through the membrane potential range at which physiological processes occur, and therefore it has been proposed that the charge movements that they represent could reflect regulatory processes in muscle (Schneider and Chandler, 1973; Chandler et al., 1976*a*). For example, it has been suggested that there is a relationship between the steeply voltage-dependent  $q_\gamma$  transition, defined either in terms of its kinetics in ON transients or its sensitivity to the contraction inhibitor tetracaine (Huang, 1981*b*; Hui, 1983), and contractile activation, either as an independent entity or after a preceding movement of the less steeply voltage-dependent and tetracaine-insensitive  $q_\beta$  (Horowicz and Schneider, 1981; Adrian and Huang, 1984*a, b*; Rakowski et al., 1985; Huang, 1986, 1987; Melzer et al., 1986). Accordingly, a clearer view of the possible relationships between the nonlinear capacity components themselves and the processes they might regulate would emerge if each component could be localized to either surface or transverse tubule membrane (Chandler et al., 1976*b*; Adrian and Huang, 1984*b*). For example, events that regulate excitation-contraction coupling should reside in transverse tubule membrane. These tubular charge movements would take place independently of events in the surface membrane, which should not be directly relevant to tubular processes such as contractile activation.

One technique for experimental separation of surface and transverse tubule membrane uses osmotic shock resulting from hypertonic glycerol withdrawal from amphibian muscle (Howell and Jenden, 1967; Krolenko, 1969). This appears to detach electrically at least part of the transverse tubule system from extracellular fluid (Fujino et al., 1961; Gage and Eisenberg 1969*a, b*; Dulhunty and Gage, 1973; Nakajima et al., 1973). Chandler et al., (1976*b*) reported a reduction in the magnitude of charge movements in fibers so treated. However, their investigation was limited by residual contractile activity that prevented accurate measurement of charge movements at larger depolarizations, and their work predated the separation of individual charge movement components (Adrian and Peres, 1979; Huang, 1981*a*; Hui, 1983). Consequently, they were not then concerned with the relative distributions of different capacity components over surface and transverse tubule membranes.

This paper describes experiments extending the approach of Chandler et al. (1976*b*). We found that cooling muscles during the detubulation procedure provided preparations with viable, detubulated surface fibers amenable to electrophysiological study for relatively long periods. A preliminary study of linear electrical properties in isotonic solutions confirmed the extent of detubulation and verified the validity of the cable analysis at the end of the fiber. To avoid any residual contractile artifacts when measuring the form and voltage dependence of charge movements even after detubulation, mechanical activity was suppressed totally by using strongly hypertonic solutions. It therefore was possible to use larger depolarizations and to explore the entire voltage range over which voltage-dependent capacitances are found in muscle. The results suggest that  $q_\gamma$  is preferentially located in the trans-

verse tubules, whereas  $q_{\beta}$  is more evenly distributed between surface and tubule membranes.

#### METHODS

A close exploration of membrane capacitance over a wide voltage range required preparations with substantially detubulated fibers, but nevertheless with stable cable constants, and they had to be viable for an hour or more.

After dissection, frog (*Rana temporaria*) sartorius muscles were mounted in a recording chamber fitted with a Peltier cooling device and were set to a center sarcomere length of 2.2–2.4  $\mu\text{m}$  using an eyepiece graticule and a Zeiss (Oberkochen)  $\times 40$  water immersion objective. Consistency of sarcomere length is important when making measurements of fiber capacitance, since actual surface membrane area relative to calculated, cylindrical area varies with sarcomere length (Dulhunty and Franzini-Armstrong, 1975). The detubulation procedure adopted was similar to that described by Gage and Eisenberg (1969b) and Chandler et al. (1976b) in that muscles were first left in a Ringer solution containing 400 mM glycerol for 50–70 min. The bathing solution was then replaced by an isotonic Ringer modified to contain 5 mM  $\text{CaCl}_2$  and 5 mM  $\text{MgCl}_2$  (Eisenberg et al., 1971) 30 min before alteration to the test solution in which electrical measurements were made. However, while in glycerol, the muscle was cooled at 10°C, and immediately after glycerol withdrawal, it was cooled to 4°C. It was found in preliminary experiments that this cooling procedure yielded surface fibers that had close to normal membrane potentials (in isotonic Ringer solution) and that survived impalement by microelectrodes well.

To investigate the possibility of pharmacological effects of glycerol on the intramembrane charge movements other than effects purely reflecting detubulation (Dulhunty and Gage, 1973), some control muscles were also exposed to glycerol at the same concentration and for the same length of time as test muscles, but the subsequent glycerol withdrawal was graded to reduce osmotic shock and avoid detubulation (cf. Jaimovitch et al., 1976). In these experiments, the glycerol Ringer was followed by 15 min in Ringer modified to contain 5 mM  $\text{CaCl}_2$ , 5 mM  $\text{MgCl}_2$  and 200 mM glycerol, and then the same solution without glycerol was used for a further 15 min before replacement by the test solution. Both the latter substitutions were also performed on cooled muscles. Finally, both intact and glycerol-shocked fibers were studied in the presence of 1 or 2 mM tetracaine to see if both detubulation and tetracaine had the same effect on the charge movements in treated fibers.

Other detubulation procedures were also explored, including that described by Chandler et al. (1976b), an inclusion of sucrose through the entire procedure, and withdrawals of both sucrose and glycerol. All these resulted in less viable fibers with less satisfactory detubulation than the procedure adopted. In *Rana temporaria* sartorius muscle, use of formamide (Argiro, 1981) resulted in leaky surface fibers with poor ( $> -12$  mV) resting potentials.

The three-microelectrode voltage clamp at the end of the fiber was used, as described more fully elsewhere (e.g., Adrian and Almers, 1976a; Adrian, 1978; Adrian and Rakowski, 1978). Preliminary experiments showed that this method more consistently gave stable records showing charge movements with slow kinetics than did either microelectrode clamping in the middle of the fiber or the use of a Vaseline gap method. Only fibers exposed on the inner surface of the muscle were studied, to increase the chances of getting consistent detubulation and also to reduce errors due to resistance of the interfiber space (Milton et al., 1985). Conventional glass microelectrodes, with a resistance of 4–10  $\text{M}\Omega$ , were inserted at standard distances of  $l = 375 \mu\text{m}$  (voltage control electrode,  $V_1$ ),  $2l = 750 \mu\text{m}$  (second voltage electrode,  $V_2$ ), and  $875 \mu\text{m}$  (current injection electrode,  $I_0$ ), respectively, from the pelvic end of the fiber. In control experiments designed to check the reliability of the three-microelectrode

clamp at the end of the fiber for obtaining cable constants, some muscles were studied with shorter (250, 500, and 625  $\mu\text{m}$ , respectively) or larger (500, 1,000, and 1,250  $\mu\text{m}$ , respectively) electrode spacings. Voltage electrodes were filled with 3 M KCl, and the current electrode with 2 M K citrate.

The membrane potential was held at  $-90$  mV. Linear membrane and cable constants were determined with 20-mV depolarizing steps 124 ms in duration imposed 500 ms after a prepulse from the  $-90$ -mV holding potential to a conditioning potential of  $-110$  mV. Values of the length constant  $\lambda$ , internal longitudinal resistance  $r_i$ , and membrane resistance of unit fiber length  $r_m$ , were calculated from steady values of  $V_1$ ,  $V_2$ , and injected current  $I_0$  at the end of the 20-mV step. The fiber diameter  $d$  and the specific membrane resistance  $R_m$  were determined using a value of the internal sarcoplasmic resistivity  $R_i$  of 391  $\Omega\text{-cm}$  in  $2.5\times$  hypertonic solution at  $2^\circ\text{C}$ , and a  $Q_{10}$  of 0.73 (Hodgkin and Nakajima, 1972*a, b*).

The membrane current through unit area of fiber surface,  $I_m(t)$ , to imposed voltage steps is given by:

$$I_m(t) = \frac{[V_1(t) - V_2(t)]d}{6l^2R_i}, \quad (1)$$

where  $t$  is time (Adrian et al., 1970; Adrian and Almers, 1974; Adrian, 1978). The capacitive charge that moved in response to an applied voltage step of size  $\Delta V_1(t)$  was computed by Simpson's Rule, integrating the transient part of the current at the beginning and after the end of each voltage step:  $\int [I_m(t) - (1/R_m)\Delta V_1(t)] dt$  (Adrian and Almers, 1974; Adrian, 1978). These integrals, and the linear cable constants calculated from the steady-state values of voltage and current, were used in control steps to calculate  $C_m$  ( $\mu\text{F}/\text{cm}^2$ ), the effective linear electrical capacity referred to unit apparent lateral fiber surface area, for both the ON and the OFF transient. We calculate apparent lateral fiber surface as the surface of a smooth circular cylinder of diameter  $d$  and length  $(3l/2)$ . These control transients, scaled for the size of the voltage step, were also subtracted from the test transients to obtain the nonlinear transients. When there was a significant baseline remaining after this subtraction, representing an extra ionic current in the test pulse, a straight line was fitted to this baseline and subtracted. Only very occasionally was it necessary to use a sloping, i.e., not horizontal, baseline for this subtraction.

The above calculations were performed on arrays of values representing  $V_1(t)$ ,  $V_1(t) - V_2(t)$  and  $I_0(t)$ , obtained by twelve-bit analog to digital conversion at an effective sampling interval of 200  $\mu\text{s}$ , after filtering through three-pole Butterworth filters set at a corner frequency of 1 kHz, and sampled using a PDP11/23 computer (Digital Equipment Corporation, Maynard, MA) with a model 502 interface (Cambridge Electronic Design, Cambridge, UK) modified by incorporating an analog-to-digital conversion silo. Five sweeps were averaged in each record when using any given pulse procedure. Linear cable constant determination was repeated at intervals of four to six test runs in the course of each experiment in order to monitor the stability and condition of the muscle fiber, and such bracketing records were used as controls for intervening test pulses when deducing nonlinear charging currents.

Earlier work had suggested that it is difficult unequivocally to achieve total detubulation by osmotic shock. Consequently, the experiments here were designed so that they could be interpreted in a manner independent of the precise degree of detubulation resulting from glycerol withdrawal. The magnitudes of linear membrane capacitances,  $C_T$ , expressed relative to lateral fiber surface areas would be affected by the amounts of transverse tubule system present, and hence would be dependent upon the degree of detubulation achieved. Therefore, these values were normalized to accessible membrane capacitance,  $C_C$ , initially without regard to the anatomical source of that capacitance. Nevertheless, an assessment of the degree of detubulation achieved by our approach is provided, incorporating an analysis en-

abling correction for membrane capacitance at the end of a muscle fiber in a three-micro-electrode clamp. Normalized values of membrane capacitance,  $C_T/C_C$ , were described where appropriate in terms of a maximum charge (also normalized to accessible membrane capacitance),  $Q_{\max}$  (nC/ $\mu$ F), steepness factor  $k$  (mV), and transition potential  $\bar{V}$  (mV) of a two-state Boltzmann system (Schneider and Chandler, 1973). The values of these parameters were obtained by a least-squares minimization of mean ( $\pm$  SE of the mean) capacitances to the appropriate hyperbolic cosine function (Adrian, 1978):

$$C_T/C_C = 1 + \frac{Q_{\max}}{2k \left[ 1 + \cosh \left( \frac{V - \bar{V}}{k} \right) \right]} \quad (2)$$

Except for studies of "subthreshold" charge, which were done using voltage steps from the holding potential directly to the test potential, the small pulse procedure of Adrian and Peres (1979) was used to obtain the voltage dependence of the membrane capacitance directly. 10-mV steps 124 ms long were superimposed on prepulse potentials that were varied in size to explore the voltage range. The resulting functions made it easier to assess directly changes not only in the amount of charge, but also the form of its dependence on voltage before and after osmotic shock.

Electrical recordings were made at 3–5°C in the following test solution: 1.25 mM  $\text{Rb}_2\text{SO}_4$ , 80 mM tetraethylammonium sulphate, 15 mM tetraethylammonium chloride, 7 mM  $\text{CaSO}_4$ ,  $2 \times 10^{-7}$  M tetrodotoxin, 3 mM HEPES buffer, pH 7.0. Experiments only studying linear electrical properties did not entail large voltage excursions from the holding potential, and were performed in this isotonic test solution. Where the full voltage range was being examined, 500 mM sucrose was added to the test solution in order to reduce contraction artifacts in the electrical records. The results presented here were obtained in the first 1.5 h after detubulation, although most preparations remained viable with good resting potentials and demonstrable charge movements even 2–3 h after glycerol withdrawal.

## RESULTS

### *Linear Electrical Properties*

Detubulated fibers in isotonic test solution had resting potentials slightly larger than untreated fibers (detubulated:  $-56.3 \pm 2.7$  mV, 25 fibers, mean  $\pm$  SE of the mean; intact:  $-47.6 \pm 0.85$  mV, 73 fibers; Student's  $t = 3.97$ ,  $P < 0.1\%$ ). Detubulation also increased specific membrane resistance  $R_m$  from  $8.10 \pm 0.97$   $\text{k}\Omega\text{-cm}^2$  (37 fibers) to  $15.24 \pm 1.86$   $\text{k}\Omega\text{-cm}^2$  (27 fibers;  $t = 3.6$ ,  $P < 0.1\%$ ), which is consistent with loss of a conductance pathway through accessible transverse tubule membrane.

Fig. 1 evaluates the electrical accessibility of the transverse tubule system by plotting effective membrane capacitance  $C_m$  determined in isotonic test solution against fiber diameter  $d$ . Three groups of fibers were studied: (a) 38 control fibers not exposed to any form of glycerol treatment, (b) 29 "detubulated" fibers subject to a single stage of glycerol withdrawal, and (c) 14 fibers exposed to glycerol but in which the osmotic shock resulting from its removal was reduced by withdrawal in two stages.

Withdrawal of glycerol in one step reduced not only the magnitude of the fiber's effective capacitance (referred to apparent fiber surface area) but also its dependence upon fiber diameter, as compared with controls. The least-squares linear

regression (A) through control data had a significant slope of  $789 \pm 13 \mu\text{F}/\text{cm}^3$  (mean  $\pm$  SE of the mean; regression coefficient  $r = 0.86$ ,  $n = 38$ ,  $P \ll 0.1\%$ ). Sudden glycerol withdrawal significantly ( $t = 22.3$ ,  $P \ll 0.1\%$ ) reduced this (B) to a nevertheless significant gradient ( $r = 0.68$ ,  $n = 29$ ,  $P \ll 0.1\%$ ) of  $357 \pm 14 \mu\text{F}/\text{cm}^3$ . However, vertical intercepts were not significantly ( $t = 0.81$ ,  $P \gg 5\%$ ) altered (from  $1.178 \pm 0.099 \mu\text{F}/\text{cm}^2$  in control to  $1.308 \pm 0.125 \mu\text{F}/\text{cm}^2$  in detubulated fibers) as would be expected had these reflected surface membrane capacitance. In contrast, two-step glycerol withdrawal left cable constants near the control values. The regres-

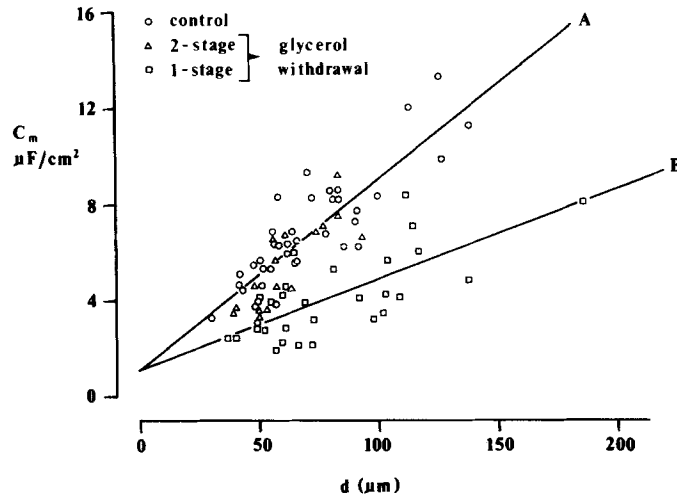


FIGURE 1. Dependence of fiber capacitance  $C_m$  ( $\mu\text{F}/\text{cm}^2$ ) referred to surface cylindrical membrane area upon electrical fiber diameter  $d$  ( $\mu\text{m}$ ) in intact (circles) and "detubulated" (squares) fibers, and fibers from muscles subject to gradual glycerol withdrawal (triangles). The clamped voltage electrode was a distance  $375 \mu\text{m}$  from the fiber end, and the muscles were in isotonic solution. Regression lines are drawn through data from intact (A) and detubulated (B) fibers. Fiber cable constants in intact fibers: length constant =  $2.06 \pm 0.16 \text{ mm}$ ,  $r_i = 9,678 \pm 1,100 \text{ k}\Omega/\text{cm}$ , diameter =  $70 \pm 4.1 \mu\text{m}$ ,  $r_m = 331.58 \pm 29.75 \text{ k}\Omega\text{-cm}$ ,  $R_m = 7.59 \pm 0.98 \text{ k}\Omega\text{-cm}^2$ ,  $C_m = 7.0 \pm 0.41 \mu\text{F}/\text{cm}^2$ ; in detubulated fibers: length constant =  $3.21 \pm 0.30 \text{ mm}$ ,  $r_i = 7,850 \pm 1,023 \text{ k}\Omega/\text{cm}$ , diameter =  $84 \pm 6.7 \mu\text{m}$ ,  $r_m = 568.4 \pm 56.3 \text{ k}\Omega\text{-cm}$ ,  $R_m = 14.9 \pm 1.8 \text{ k}\Omega\text{-cm}^2$ ,  $C_m = 4.3 \pm 0.32 \mu\text{F}/\text{cm}^2$ ; and two-stage glycerol withdrawal: length constant =  $2.4 \pm 0.28 \text{ mm}$ ,  $r_i = 11,696 \pm 1,462 \text{ k}\Omega/\text{cm}$ , diameter =  $59.5 \pm 4.3 \mu\text{m}$ ,  $r_m = 622.02 \pm 106.6 \text{ k}\Omega\text{-cm}$ ,  $R_m = 11.52 \pm 2.14 \text{ k}\Omega\text{-cm}^2$ ,  $C_m = 5.1 \pm 0.42 \mu\text{F}/\text{cm}^2$ .

sion slope ( $784 \pm 49 \mu\text{F}/\text{cm}^3$ ,  $n = 14$ ) and intercept ( $1.061 \pm 0.306 \mu\text{F}/\text{cm}^2$ ) were not then significantly different ( $t = 0.13, 0.46$ ,  $P \gg 5\%$ ) from those obtained for control fibers (curve not drawn for two-step withdrawal).

The determination of effective capacitance,  $C_m$ , from the integral of the transient current does not depend on assuming any particular equivalent circuit for the muscle fiber membrane (Adrian and Almers, 1974). However, in order to make any statements about the quantity of charge movement per unit area of muscle fiber membrane, or to estimate the degree of detubulation achieved in glycerol-treated

fibers from linear capacitance data, it is necessary to assume a specific model for the muscle membranes. In the case of the end of the fiber voltage clamp used here, that model should include both the lateral surface membrane and the tubule membranes from the end of the fiber to a distance of  $(3l/2)$  from the end of the fiber (Adrian et al., 1970), plus the membrane covering the myotendon junction at the end of the fiber.

In the model of Adrian and Almers (1974) and Adrian (1978), the current flow, estimated by the potential difference between the two voltage-measuring microelectrodes (Eq. 1), charges all of this capacitance to an average potential of  $V_1$ , the pulse command potential. Their analysis assumes that there is no current flow through the end of the fiber. Milton et al. (1985) determined the electrical properties of the end of the fiber by a direct measurement of the end of the fiber admittance, and found it to have a specific conductance, per unit fiber cross-sectional area, of  $0.5 \text{ mS/cm}^2$ . While this specific conductance is more than twice that of the fiber surface membrane, also expressed per unit area, the cross-sectional area of the end of even a relatively large fiber ( $100\text{-}\mu\text{m}$  diameter) is only  $\sim 4\%$  of the apparent lateral surface area of the same fiber, at our standard electrode spacing. Therefore,  $<10\%$  of the measured steady-state current is expected to flow through the membrane at the end of the fiber. This suggests that the assumption of no steady state current through the end of the fiber is not a bad one.

In contrast, the capacitance at the end of a fiber is greatly influenced by a large membrane area found at the myotendon junction (50 times the cross-sectional area of the fiber: Eisenberg and Milton, 1984) which must be added to the capacitance of the lateral fiber surface plus that of the transverse tubules to get the total fiber capacitance. Therefore, the total effective capacitance,  $C_m$ , of a length  $(3l/2)$  at the end of a fiber of diameter  $d$  includes a geometric term for the cross-sectional area of the end of the fiber ( $\pi d^2/4$ ) plus another term for the surface area of transverse tubules in unit volume of fiber ( $\rho/\zeta$ ) times the volume of that length of fiber ( $3\pi d^2 l/8$ ), ( $\zeta$  is the volume to surface ratio of transverse tubules, and  $\rho$  is their volume fraction in the fiber). When each of these geometric terms is multiplied by the appropriate specific capacitance, the total effective linear capacitance of the voltage-clamped part of the fiber, normalized to its apparent lateral surface area, is given by:

$$C_m = C_s + \left(\frac{\rho d}{4\zeta}\right) C_t + \left(\frac{d}{6l}\right) C_e, \quad (3)$$

where  $C_s$ ,  $C_t$ , and  $C_e$  are the specific capacitances, in  $\mu\text{F/cm}^2$ , of the lateral surface, transverse tubules, and end of the fiber, respectively. Using values of  $\rho = 0.003$ ,  $\zeta = 10^{-6} \text{ cm}$  (Peachey, 1965), and  $l = 375 \mu\text{m}$ , the diameter-dependent terms in Eq. 3 become  $750dC_t$  and  $4.44dC_e$  ( $\mu\text{F/cm}^2$ ).

For a  $100\text{-}\mu\text{m}$  diameter fiber, and using values of  $C_s = 2.3 \mu\text{F/cm}^2$ ,  $C_t = 0.77 \mu\text{F/cm}^2$ , and  $C_e = 50 \mu\text{F/cm}^2$  (Milton et al., 1985), the capacitance at the end of the fiber, normalized to the apparent lateral fiber surface area, is  $2.2 \mu\text{F/cm}^2$ , only slightly less than that of the lateral surface itself ( $2.3 \mu\text{F/cm}^2$ ), and an appreciable fraction of the capacitance of the transverse tubule system normalized in the same

way ( $5.78 \mu\text{F}/\text{cm}^2$ ). To ignore the contribution to  $C_m$  of the fiber end surface, therefore, leads to an appreciable error.

The sum of the coefficients of the diameter-dependent terms in Eq. 3,  $750C_t + 4.44C_e$ , represents the slope of a plot of  $C_m$  against  $d$ , as in Fig. 1. For an intact fiber, with  $l = 375 \mu\text{m}$  and using the values of transverse-tubule and end-specific capacitances given above, a slope of  $800 \mu\text{F}/\text{cm}^3$  would be predicted, which is in close agreement both with earlier results (e.g., Adrian and Huang, 1984*b*) and with present results for intact fibers, suggesting that the model assumed here represents a good description of the membrane distribution at the end of the fiber.

As a further check that the linear capacitance obtained by the method used here agrees with values expected for the model assumed, and to provide an independent check on the values assumed for  $C_t$  and  $C_e$ , we determined the linear electrical properties of some fibers using different values of  $l$ , the electrode spacing. These included the spacing used for curve A of Fig. 1 ( $375 \mu\text{m}$ ) as well as a larger value ( $500 \mu\text{m}$ ) and a smaller one ( $250 \mu\text{m}$ ). The slopes of plots of  $C_m$  against  $d$  for the three values of  $l$  were plotted against the inverse of  $l$ . From the slope ( $C_e/6$ ) and intercept ( $\rho C_t/4\zeta$ ) of this plot, we calculate values of  $C_t = 0.84 \mu\text{F}/\text{cm}^2$  and  $C_e = 34 \mu\text{F}/\text{cm}^2$ , which is in reasonable agreement with values obtained from more extensive studies using impedance analysis over a wide frequency range ( $0.77 \mu\text{F}/\text{cm}^2$  and  $50 \mu\text{F}/\text{cm}^2$ , respectively; Milton et al., 1985). Since our experiments at the alternate electrode spacings involved a smaller number of fibers relative to the number we studied at the standard electrode spacing, and because we think that caution in using numbers based on extrapolated graphs is prudent, we will use the numbers obtained by Milton et al. (1985) for the calculations done in this paper. However, based on the similarity of our results with their's, we feel confident that our values for effective linear capacitance are reasonably sound, and that we are justified in using them for normalizing nonlinear capacitance as well as when estimating the proportional detubulation after glycerol treatment.

#### *Extent of Detubulation*

Since the slope of a capacitance-diameter plot for a completely detubulated fiber ( $C_t = 0$ ) would be  $222 \mu\text{F}/\text{cm}^3$ , we can estimate the proportional detubulation for a partially detubulated fiber with a measured effective linear capacitance of  $C_m$  ( $\mu\text{F}/\text{cm}^2$ ) by:

$$0 \leq \frac{C_s + 800d - C_m}{578d} \leq 1.0. \quad (4)$$

This computation confirmed an absence of significant detubulation in control fibers ( $0.019 \pm 0.049$ ;  $n = 38$ ). Values of surface capacitance ( $C_s$ ) range from the intercepts of the present regression lines ( $\sim 1.18 \mu\text{F}/\text{cm}^2$ ), which are similar to those reported by Hodgkin and Nakajima ( $0.9 \mu\text{F}/\text{cm}^2$ : 1972*a, b*), to higher values obtained by other methods ( $2.3 \mu\text{F}/\text{cm}^2$ : Gage and Eisenberg, 1969*a*; Milton et al., 1985). These yield relative detubulations between  $0.75 \pm 0.05$  and  $1.02 \pm 0.06$ , respectively, for the detubulated group of fibers in this study. Degree of detubulation did not significantly correlate with fiber diameter (controls:  $r = -0.035$ ,  $t = 0.210$ ,  $P \gg 5\%$ ; detubulated:  $r = -0.00062$ ,  $t = 3.1 \times 10^{-3}$ ,  $P \gg 5\%$ ). Thus,



whereas the dependence upon diameter of capacitances of untreated fibers agreed with earlier morphological (Peachey, 1965) and electrical (Milton et al., 1985) findings for fibers with intact transverse tubular systems, treated fibers were at least 75% detubulated.

#### *Detubulation and "Subthreshold" Charge Movement*

"Subthreshold" charge (charge moving between voltages of  $-90$  and  $-60$  mV in the absence of detectable mechanical activity) has been suggested to represent transitions necessary to later charge movements more directly involved in excitation-contraction coupling (Melzer et al., 1986). A tubular location for such preliminary charge movement would be compatible with such a hypothesis. To explore this,

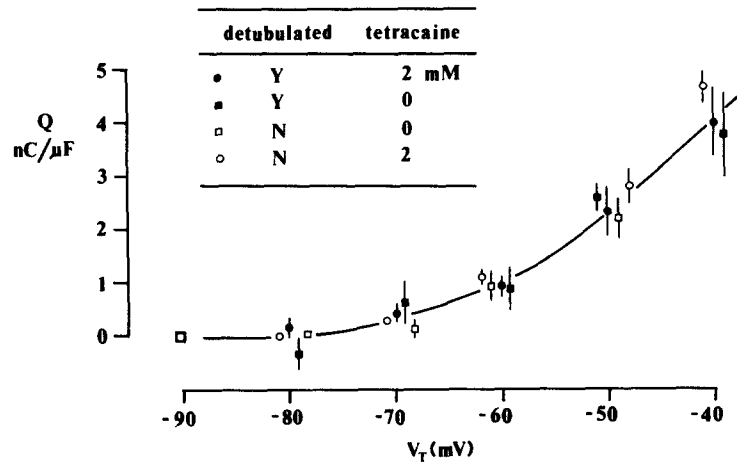


FIGURE 2. Voltage dependence of "subthreshold" charge movement in intact and detubulated fibers in isotonic solutions, and in the presence and absence of 2 mM tetracaine. Voltage steps were made to membrane potentials at 10-mV increments from the  $-90$ -mV holding potential, but the symbols are slightly offset horizontally for clarity. Contractile threshold in intact fibers was  $\sim 45$  mV in this series. Intact fibers: length constant =  $3.53 \pm 0.31$  mm,  $r_i = 4,298.6 \pm 915.4$  k $\Omega$ /cm, diameter =  $97.5 \pm 5.6$   $\mu$ m,  $r_m = 497.2 \pm 68.1$  k $\Omega$ -cm,  $R_m = 15.11 \pm 2.44$  k $\Omega$ -cm $^2$ ,  $C_m = 10.43 \pm 0.94$   $\mu$ F/cm $^2$ . Detubulated fibers: length constant =  $4.18 \pm 0.95$  mm,  $r_i = 7,321 \pm 3,065$  k $\Omega$ /cm, diameter =  $107 \pm 21.5$   $\mu$ m,  $r_m = 555.7 \pm 87.3$  k $\Omega$ -cm,  $R_m = 19.18 \pm 4.9$  k $\Omega$ -cm $^2$ ,  $C_m = 5.4 \pm 0.63$   $\mu$ F/cm $^2$ .

large test voltage steps from a holding potential of  $-90$  mV to a range of voltages between  $-80$  and  $-40$  mV were applied to both intact and detubulated fibers in isotonic solutions, in the presence and absence of 2 mM tetracaine, so that comparisons could be made not only in terms of "subthreshold" charge but also its tetracaine sensitivity.

Fig. 2 plots voltage-dependent charge movement (mean  $\pm$  SE of the mean) relative to accessible linear capacitance of each fiber at  $-90$  mV. Charge movement increased with depolarization from  $-90$  mV to  $\sim 4$  nC/ $\mu$ F at a potential of  $-40$  mV, in both control and detubulated fibers. The addition of tetracaine did not alter the

charge-voltage curves in either control or detubulated fibers, which is consistent with most of the "subthreshold" charge being made up of tetracaine-resistant ( $q_{\beta}$ ) charge. A steady-state charge residing primarily in the transverse tubule system, would have been diminished by detubulation, but Fig. 2 shows that this was not the case. Since charge-voltage curves normalized to effective membrane capacitance were not altered by detubulation, whether in the presence or absence of tetracaine, this suggests an equal representation of "subthreshold" charge on both surface and transverse tubule membrane.

*Charge Movements in Fibers with and without Abrupt Glycerol Withdrawal*

Fig. 3 compares the voltage dependence and kinetics of charge movements in glycerol-treated muscle fibers in a hypertonic tetraethylammonium-containing solution with and without osmotic shock. Before obtaining the records in the detubulated

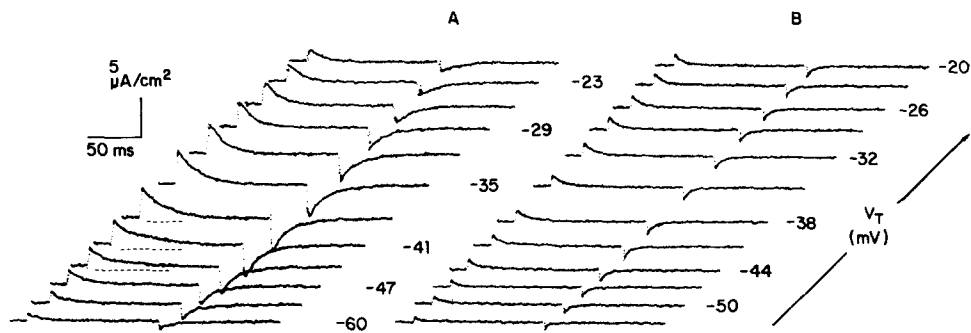


FIGURE 3. Examples of charge movements obtained in hypertonic test solutions in response to small, 10-mV steps at depolarizing voltages in fibers previously exposed to (A) graded, and (B) abrupt glycerol withdrawal. Numbers next to the records are the membrane potentials ( $V_T$ , mV) to which the fiber was depolarized by the 10-mV steps, and are the same for corresponding records in intact and detubulated fibers. Dotted lines under three of the current traces for the intact fiber indicate the slow phase identified with  $q_{\gamma}$ .

muscle, action potentials were elicited by current-clamp pulses applied to several surface fibers while the muscle was still in isotonic Ringer. When a contraction did occur, it was so weak that even electrodes in the end of a relatively slack fiber were not dislodged, confirming that significant detubulation had been achieved. Muscles were then put into hypertonic test solution and studied using 10-mV pulses to test levels  $V_T$ , superimposed 500 ms after a voltage step to prepulse potentials altered in close (often 3 mV) increments. Fig. 3 A illustrates charge movements in intact fibers that included not only rapid ( $q_{\beta}$ ) charging transients at small depolarizations but also more prolonged and gradual ( $q_{\gamma}$ ) decays at some voltages. The latter were prolonged over 50–70 ms at a membrane potential of  $-44$  mV (see also Fig. 4), but even small (3–6 mV) further depolarization resulted in more rapid charge transfers. These merged with the earlier  $q_{\beta}$  monotonic decay by  $-35$  mV. This marked dependence of the duration of the charging current upon voltage makes it unlikely that it results from purely linear tubular delays. In contrast, OFF transients were monotonic

decays whose magnitude and time course varied relatively continuously with voltage (cf. Huang, 1984).

Charge movements in detubulated fibers (Fig. 3 *B*) were smaller, when normalized to the apparent lateral surface area of the fiber, confirming a reduction in total charge with detubulation. Charge movements in detubulated fibers also did not show slow kinetics at a circumscribed set of voltages. Transients at all voltages were monotonic decays with symmetrical ON and OFF kinetics, complete within  $\sim 5$  ms. They accordingly resembled  $q_{\beta}$  currents reported earlier (Adrian and Peres, 1979; Huang, 1982; Hui, 1983). Delayed transients were not found in detubulated fibers even with close exploration of membrane potentials in 3-mV increments.

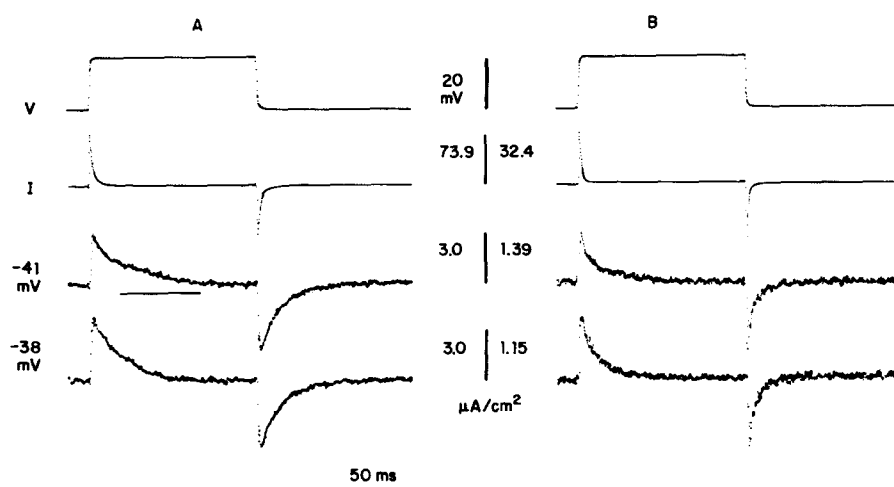


FIGURE 4. Time course of the imposed voltage clamp steps ( $V$ ) at the control ( $-90$  mV) membrane potential, the resulting current transients ( $I$ ), and charge movements to 10-mV steps to  $-41$  and  $-38$  mV test potentials in fibers previously exposed to (*A*) graded and (*B*) abrupt glycerol withdrawal. Each of the lower three records in (*B*) has been scaled vertically to the maximum ON value of the corresponding record in *A*. The time constants of control ( $-90$  mV) currents in either *A* (2.6 ms) or *B* (1.6 ms) are short relative to the time courses of either early or late (horizontal bar in *A*) charge movements.

The current transients shown in Fig. 3 were normalized to a square centimeter of apparent lateral fiber surface, which results in smaller transients for detubulated fibers than for intact fibers. To provide a better illustration of the time courses of these transients for intact and detubulated fibers, two of the records for the detubulated fiber in Fig. 3 *B* have been replotted to the same peak height as the corresponding records in Fig. 3 *A* for the intact fiber. These are displayed in Fig. 4 *A* and *B* along with typical total current and voltage records plotted with a similar peak height and the same time scale for each fiber. The slow phase in the record for the intact fiber at  $-41$  mV is marked with an underlying bar (Fig. 4 *A*). At most, only a minimal slow transient is seen in the corresponding records for the detubulated fiber (Fig. 4 *B*); in many fibers, no slow transient was apparent. It can also be seen that the full control current records are much too fast to account for the slowness

of any of the transients. Therefore, tubular delays *per se* cannot account for the slow phase observed in ON transients at certain voltages in intact fibers.

#### *Comparisons of Capacitance-Voltage Curves*

The results shown in Figs. 3 and 4 are based on the visual observation of slow components in the recorded charge movement transients from individual fibers as evidence for the presence or absence of  $q_\gamma$ . Independent of any interpretation based on the kinetics of the charge movement, the total amount of steady-state capacitance and its dependence upon voltage were reduced in detubulated fibers. The capacitance was measured from the integral of the transient current in response to a 10-mV step to the test potential in a solution (Adrian and Almers, 1976*a, b*) that minimized ionic conductances and consequently potential decrement in the transverse tubule system. Additionally, capacitance was normalized to a reference capacitance value obtained at  $-90$  mV. This approach therefore yields a dimensionless value of total capacitance, referred to accessible linear fiber membrane capacitance, independent of the equivalent circuit of the system (Adrian and Almers, 1974).

TABLE I  
*Cable Constants for Detubulated and Tetracaine-treated Fibers*

Condition	$n$	$d$	$r_i$	$R_m$	$\tau_m$	$\lambda$	$c_m$
		$\mu\text{m}$	$\text{k}\Omega/\text{cm}^2$	$\text{k}\Omega\text{-cm}^2$	$\text{k}\Omega\text{-cm}$	$\text{mm}$	$\mu\text{F}/\text{cm}^2$
Intact, 1 mM tetracaine	3	62.6 $\pm 2.7$	12,500 $\pm 1,100$	5.2 $\pm 2.1$	279 $\pm 120$	1.38 $\pm .24$	13.30 $\pm 0.95$
Detubulated, no tetracaine	3	66.7 $\pm 5.9$	11,600 $\pm 1,900$	16.2 $\pm 4.3$	768 $\pm 177$	2.62 $\pm .47$	8.51 $\pm 2.40$
Detubulated, 1 mM tetracaine	6	62.3 $\pm 3.8$	12,800 $\pm 1,330$	11.2 $\pm 2.9$	586 $\pm 160$	2.07 $\pm .26$	7.73 $\pm 0.46$

Fibers included were selected from those used for the experiments shown in Figs. 5 and 6. Only fibers whose diameters were between 50 and 70  $\mu\text{m}$  are included in this table.

Using this approach, we analyzed in detail the membrane capacitance of groups of muscle fibers studied after different treatments, including detubulation and the addition of 1 mM tetracaine to the test solution, which eliminates  $q_\gamma$  in normal muscle fibers, leaving only the tetracaine-resistant  $q_\beta$  (Huang, 1982; Hui, 1983). In all cases charge movements were examined in hypertonic solutions to avoid residual contractile artifacts. Fiber diameters were deduced by a cable analysis of 20-mV pulses obtained at the  $-90$ -mV control voltage, as described under Methods.

To evaluate the physiological state of the membranes of the fibers under different forms of treatment, we compared the linear cable constants obtained for a selected group of fibers in each of the three experimental conditions in which the effects of detubulation and tetracaine on fiber capacitance were studied. The fibers included in this comparison were selected from all fibers studied as those whose diameters fell into the range of 50–70  $\mu\text{m}$ . This selection, based on fiber diameter, was made so that comparisons of cable constants could be made for fiber groups with approximately the same proportions of surface and tubule membranes before detubula-

tion. Table I shows that detubulated fibers with tetracaine present have roughly the same length constants and reasonable values of specific membrane resistance, compared with detubulated fibers without tetracaine. Although tetracaine did reduce mean membrane specific resistance ( $R_m$ ) for detubulated fibers from  $\sim 16$  to  $\sim 11$   $\text{k}\Omega\cdot\text{cm}^2$ , this was still well above the value of  $\sim 5$   $\text{k}\Omega\cdot\text{cm}^2$  obtained for intact fibers with tetracaine present. This indicates that 1 mM tetracaine does not produce highly leaky fiber membranes in frog fibers studied with microelectrodes, as it does in the case of mammalian fibers studied using the Vaseline gap method (Lamb, 1986).

Curve A of Fig. 5 plots mean capacitance ratios  $\pm$  SE of the mean from seven fibers previously subjected to graded glycerol withdrawal and studied in the absence of tetracaine. The membrane capacitance showed a marked voltage dependence

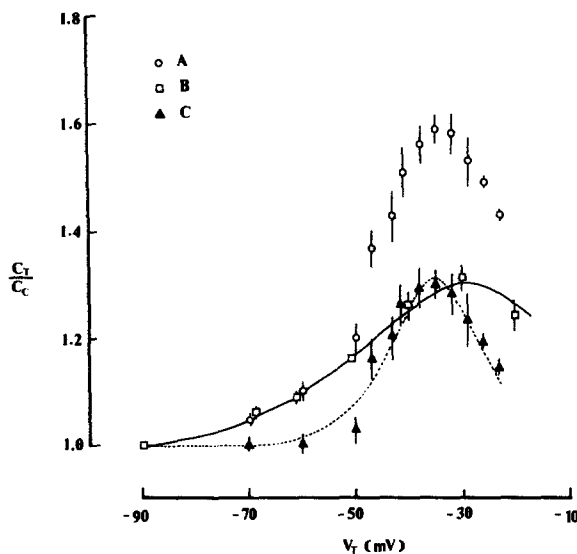


FIGURE 5. Voltage dependence of mean ( $\pm$  SE of the mean) capacitance ratios in fibers subject to two-stage glycerol withdrawal measured in hypertonic solutions in the absence (A), and the presence (B) of 1 mM tetracaine. The points in (C) were obtained from the differences between the data points (A) and the least-squares Boltzmann fit (continuous line) through the data in B. The dashed line is a least-squares fit of a Boltzmann function to the points in C. Capacitances are normalized to accessible control values obtained at  $-90$  mV. Fiber diameters (A:  $80.5 \pm 5.12$   $\mu\text{m}$ , 7 fibers; B:  $75.3 \pm 4.4$   $\mu\text{m}$ , 14 fibers) in the two groups were similar.

resembling earlier reports for fibers not treated with glycerol (Adrian and Almers, 1976a; Adrian and Peres, 1979; Huang 1982). Capacitance first increased gradually with depolarization beyond  $-90$  mV. Then there was a sharp rise beyond  $-50$  mV to reach a peak capacitance ratio of  $\sim 1.6$  near  $-35$  mV. Capacitance then decreased with stronger depolarization. Tetracaine (1 mM) abolished the marked increase in capacitance seen in control fibers with depolarization beyond  $\sim -50$  mV (Fig. 5 B). The maximum capacitance ratio occurred at a membrane potential of  $\sim -30$  mV, but had a far smaller value of 1.3. The shape of the function was more gradual than what would have resulted from a simple scaling down of the curve without tetracaine. This change in both magnitude and shape of the capacitance-voltage relationship was in agreement with earlier results (Huang, 1982; Hui, 1983).

A description of the results on tetracaine-treated control fibers in terms of a Boltzmann function suggested a  $Q_{\max}$  value of  $16.0 \pm 2.29$  nC/ $\mu$ F, with  $\bar{V} = -29.7 \pm 0.24$  mV and  $k = 13.3 \pm 1.47$  mV.

Further analysis of the above data provided a separation of charge movement components in agreement with earlier work (Adrian and Peres, 1979; Duane and Huang, 1982). Fig. 5 C was obtained by subtracting the fitted Boltzmann function obtained for Fig. 5 B (continuous line) from the original data of Fig. 5 A in order to deduce the characteristics of tetracaine-sensitive charge alone. The interrupted line is the least-squares fit of a Boltzmann function to the differences, which yielded parameters ( $Q_{\max} = 7.04 \pm 0.49$  nC/ $\mu$ F;  $\bar{V} = -35.2 \pm 0.61$  mV;  $k = 5.68 \pm 0.51$  mV) in close agreement with other determinations for the  $q_{\gamma}$  capacitance component (Duane and Huang, 1982; Hui, 1983). Note the relatively poor fit to the data at

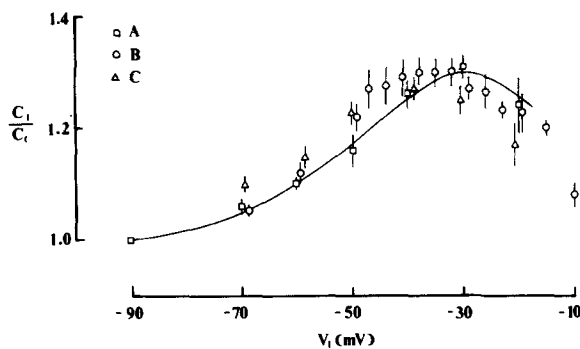


FIGURE 6. Voltage dependence of mean ( $\pm$  SE of the mean) capacitance measured in hypertonic solutions in (A) intact fibers in the presence of 1 mM tetracaine, and in detubulated fibers in the absence (B) and in the presence (C) of 1 mM tetracaine. The continuous line is the least-squares Boltzmann fit through A as first represented in Fig. 5. Capacitances are normalized to accessible control values at  $-90$  mV. Fiber diameters (A:  $75.3 \pm 4.4$   $\mu$ m, 14 fibers; B:  $82.9 \pm 2.3$   $\mu$ m, 9 fibers; and C:  $75.0 \pm 6.9$   $\mu$ m, 11 fibers) in the three groups were similar.

$\sim -50$  mV, where the measured capacitance rises more steeply than does the fitted curve, as observed earlier for  $q_{\gamma}$  by Hui (1983).

Capacitance-voltage curves also were compared in detubulated fibers in the presence and absence of tetracaine. Appreciable representation of  $q_{\gamma}$  either on surface membrane, or on membrane remaining electrically accessible from the surface even after osmotic shock, then would produce a further fall in membrane capacity with tetracaine treatment even in a previously detubulated fiber. In contrast, were  $q_{\gamma}$  to reside principally in transverse tubule membrane electrically detached by the osmotic treatment, there would be no further decrease in capacitance with the addition of drug in detubulated fibers. Fig. 6 plots the voltage dependence of membrane capacity in detubulated fibers in the absence (B) and presence (C) of tetracaine, along with the data (A) from Fig. 5 B for control fibers treated with tetracaine. There are no significant differences in the data for the three conditions, suggesting that detubulation and tetracaine treatment, applied either together or separately,

have the same effect on charge movements, i.e., they eliminate  $q_\gamma$  and leave the full amount of  $q_\beta$  intact when normalized to accessible membrane capacitance. This provides evidence that  $q_\gamma$  is located principally in the transverse tubule membranes, which are isolated electrically from the fiber surface by detubulation.

#### DISCUSSION

Adrian and Huang (1984*b*) observed that capacitance attributable to tetracaine-sensitive ( $q_\gamma$ ) but not to tetracaine-resistant ( $q_\beta$ ) charge increased with fiber diameter, suggesting that these had different relative distributions over transverse tubule and surface membrane. The experiments reported here examined the effects of osmotic shock from sudden glycerol withdrawal on charge movements in order to investigate further the anatomical location of these charge movements with respect to the surface and transverse tubule membranes of the muscle fiber. Whatever the precise effect of this treatment (see Dulhunty and Gage, 1973; Nakajima et al., 1973), a linear cable analysis including the membrane covering the end of the fiber suggested that the procedure used here yielded preparations with viable surface fibers whose transverse tubule systems were largely electrically inaccessible from the external solution. This allowed us to study charge distribution in fibers with complete transverse tubule systems present as well as fibers with most of their transverse tubule membrane eliminated from the electrical records. Membrane capacitance was explored over a range of voltages. It was expressed as a dimensionless quantity independent of fiber geometry by normalization to accessible fiber membrane capacitance measured at the holding potential (see Methods). If all intramembrane charge were distributed evenly over surface and tubule membrane, partial or total detachment of the transverse tubules would not alter either this capacitance ratio or the form of its voltage dependence, whatever the precise degree of detubulation. On the other hand, both the size and the shape of the dependence of capacitance on voltage would alter with detubulation if any component of the charge were to be located preferentially either in the transverse tubules or on the surface of the fiber. Thus we have been able to use detubulated fibers to evaluate the specific distribution of different components of charge, even without knowing precisely the degree of detubulation achieved.

We include here some illustrations of charge movement transients recorded from intact and detubulated fibers (Figs. 3 and 4), for comparison of the kinetics of charge movements in fibers with and without attached transverse tubules. The result was a significant reduction or complete absence of slow transients identifiable with  $q_\gamma$  in detubulated fibers. Any small, residual slow transient seen in detubulated fibers could be explained if that particular fiber was not fully detubulated. Since it is difficult to quantitate these slow transients by visual inspection of the records, especially in detubulated fibers, we also measured the nonlinear capacitance by numerical integration of current transients, and normalized this to the linear capacitance determined at the holding potential of  $-90$  mV. This provides quantitative measures of nonlinear capacitance that can be treated statistically for groups of fibers treated in the same way experimentally. Thus, all of our conclusions can be based on these quantitative measurements rather than on the visualization of slow kinetic components in transients.

In the experiments reported here, the detubulation procedure abolished a portion of the charge, and reduced the steepness of the voltage dependence of membrane capacitance. However, neither the quantity of charge nor its voltage dependence was further altered by tetracaine in fibers that had been detubulated. Using  $q_\gamma$ 's definition of being the tetracaine-sensitive component of charge (Huang, 1981a; Hui, 1983), these results make it seem likely that  $q_\gamma$  is concentrated in the transverse tubule system, and either absent from the surface membrane or present in such a low concentration that we could not detect it. In contrast to  $q_\gamma$ , the faster and tetracaine-resistant  $q_\beta$  charge movements persisted in detubulated fibers, and at the same level as in intact fibers, when expressed normalized to accessible membrane capacitance. The distribution of "subthreshold" charge similarly was not significantly affected by detubulation when normalized in the same way. Additionally, tetracaine did not affect "subthreshold" charge in either control or detubulated fibers. These results, using quantitative estimates of charge movements based on integration of current transients, are in complete agreement with the results that were based on visual evaluation of the kinetics of the transients, i.e., that  $q_\gamma$  is localized in the transverse tubule system membranes.

The simplest interpretation of these results concerning the distribution of  $q_\beta$  in surface membranes is that it is evenly distributed between membranes on the lateral surfaces of the fiber and the membranes at the end of the fiber in the myotendon junction. Since the areas of these two structurally distinct regions of membranes are roughly equal (see page 571), and since these membranes all persist after detubulation, we could not in fact distinguish between an even distribution of  $q_\beta$  in end and lateral surface membranes and a situation in which  $q_\beta$  was absent from one of these classes of membranes and twice as dense in the other, or even some intermediate between these extremes. However, an even distribution of  $q_\beta$  over end, lateral surface, and transverse tubule membranes seems to be the best interpretation of our results given the present experimental evidence.

To be sure that differences between records obtained from detubulated and from control fibers could be explained by the detubulation procedure alone without requiring other effects of glycerol upon charging currents, additional control experiments reported here used muscles also exposed to glycerol, but with the glycerol withdrawn in stages rather than abruptly in order to reduce osmotic shock. The cable constants of such fibers and both the magnitude and the voltage dependence of their membrane capacitance closely resembled that seen in untreated, intact fibers. This makes it likely that the  $q_\gamma$  charge was removed by glycerol withdrawal through its osmotic effects in causing detubulation rather than as a result of cross-linking membrane components (Buckingham and Staehelin, 1969) or any other chemical or pharmacological effects, such as reported by Dulhunty and Gage (1973) for toad fibers.

In an earlier paper, Chandler et al. (1976b) studied nonlinear capacitance in frog skeletal muscle fibers using glycerol withdrawal at room temperature. They reported that detubulation was only 40–60% complete, and they found that proportionately more (two-thirds of the total) nonlinear capacitance was removed by their treatment than was the linear capacitance. These results could be reconciled with our results by noting that they worked closer to the end of the fiber than we did, and they did not take into account the capacitance at the end of the fiber, which can have a



capacitance as large as that of the lateral fiber surface, even at our larger electrode spacing. Thus, it seems likely that a significant amount of the linear capacitance remaining in their fibers after glycerol treatment may have been due to the membrane at the ends of the fibers, not to transverse tubule membrane, and consequently that their treated fibers may have been more detubulated than they calculated.

Our detubulation results suggest that transverse tubule and surface membranes of skeletal muscle contain different mixtures of the major ( $q_\beta$  and  $q_\gamma$ ) intramembrane charge components. Since the  $q_\gamma$  charge, which produces the steep voltage dependence of capacitance (Adrian and Peres, 1979; Huang, 1982) virtually disappears with detubulation, we conclude that  $q_\gamma$  is preferentially localized in transverse tubule membrane, which is consistent with a possible role in excitation-contraction coupling. However, detubulation spared the faster  $q_\beta$  charging current in a way that suggested an equal representation over surface and transverse tubule membrane. These results are consistent with earlier pharmacological and kinetic studies that suggested at least two causally independent charge movement components (Adrian and Huang 1984a; Huang, 1986, 1987). Our results also suggest that a significant proportion of "subthreshold" charge (Melzer et al., 1986) is present on surface membrane. It is therefore likely that at least some of this latter charge may not be related directly to contractile activation in amphibian muscle, though it cannot be ruled out that the part of this charge that resides in the transverse tubule system could be required to move before  $q_\gamma$  moves.

The maximum quantity of  $q_\gamma$  given in the literature falls between 5 and 15 nC/ $\mu$ F (Huang, 1982; Hui, 1983; present observations). A valency of 4, deduced from our values for  $k$ , gives an upper limit of 190–240  $q_\gamma$  charge groups/ $\mu$ m<sup>2</sup> of transverse tubule membrane, assuming that all of  $q_\gamma$  is in the tubule membranes and further assuming a tubular specific membrane capacitance of between 0.8 and 1.0  $\mu$ F/cm<sup>2</sup>. This is considerably less than what is predicted when one bases the calculation on the entire charge movement (Chandler et al., 1976a), and also is less than the numbers of "feet" in triad complexes ( $\sim$ 800/ $\mu$ m<sup>2</sup> total transverse tubule membrane), based on electron microscopic observations (Franzini-Armstrong, 1975). However this need not exclude a correlation between either  $q_\gamma$  charge movements or contractile activation and observed anatomical structures. For example, it is possible that not all the "feet" may be at any one time be active and generate charge movements.

One conclusion that seems clear from our results is that  $q_\beta$  and  $q_\gamma$  are necessarily due to two different molecules, or if they are in the same molecule, it must be in a different environment or state in the transverse tubule system compared with the surface membrane, since the two charges have different anatomical distributions. Furthermore, our results make it likely that  $q_\gamma$ , and not  $q_\beta$ , represents the voltage-sensing step in the transverse tubule membrane that initiates excitation-contraction coupling, regardless of the nature of the subsequent steps leading to calcium release from the sarcoplasmic reticulum. Therefore, it may be of interest to review briefly what the subsequent steps might be.

One possibility is that a molecule in the transverse tubule membrane, perhaps the dihydropyridine receptor recently demonstrated by Curtis and Caterall (1984), moves in response to the change in transmembrane potential, and, via a mechanism

like that proposed by Chandler et al. (1976*b*), mechanically influences a molecule or molecules in the sarcoplasmic reticulum membrane to open calcium channels. This idea has been put forth by Rios and Brum (1987), who recently reported that both total charge movement and internal calcium transients are reduced in frog muscle fibers in the presence of 500 nM nifedipine, though the pulse procedure used did not allow them to distinguish between  $q_{\beta}$  and  $q_{\gamma}$ . The density of receptor molecules for 1,4-dihydropyridines recently has been studied using binding measurements in frog sartorius muscles by Schwartz et al., (1985), who calculated a density of 230 binding sites/cm<sup>2</sup> transverse tubule membrane. This is in good agreement with our calculated density of  $q_{\gamma}$  charge movements. Alternatively, the voltage-sensor in the transverse tubule membrane could be a molecule that produces or releases a transmitter, perhaps inositol 1,4,5-triphosphate (Vergara et al., 1985), which would then act to open sarcoplasmic reticulum calcium channels. The observation that 0.5 mM tetracaine apparently inhibits phosphatidylinositol phosphorylation in transverse tubule membranes isolated from frog skeletal muscles is in agreement with this idea (Hidalgo et al., 1986). Further information is needed before these alternatives can be evaluated, but our results suggest strongly that the molecule that senses the voltage change in the transverse tubule membrane and initiates the next step in excitation-contraction coupling is the molecule that produces the charge movement  $q_{\gamma}$ , and that its density in transverse tubule membranes of frog muscle is not more than  $\sim 250/\mu\text{m}^2$ .

We thank Prof. R. H. Adrian for many helpful discussions during the course of the work, and Mr. W. Smith for skilled assistance. We also thank W. Almers and W. K. Chandler, who read the manuscript and made helpful suggestions. Mrs. Teresa Smith kindly prepared the manuscript.

L. D. Peachey was a Royal Society Visiting Fellow. Some of the equipment used was also provided by the Royal Society. This work was supported in part by the Muscular Dystrophy Association and the Henry M. Watts Neuromuscular Disease Research Center.

*Original version received 22 January 1988 and accepted version received 26 August 1988.*

#### REFERENCES

- Adrian, R. H. 1978. Charge movement in the membrane of striated muscle. *Annual Review of Biophysics and Bioengineering*. 7:85–112.
- Adrian, R. H., and W. Almers, 1974. Membrane capacity measurements on frog skeletal muscle in media of low ionic content. *Journal of Physiology*. 237:573–605.
- Adrian, R. H., and W. Almers. 1976*a*. The voltage dependence of membrane capacity. *Journal of Physiology*. 254:317–338.
- Adrian, R. H., and W. Almers. 1976*b*. Charge movement in the membrane of striated muscle. *Journal of Physiology*. 254:339–360.
- Adrian, R. H., W. K. Chandler, and A. L. Hodgkin. 1970. Voltage clamp experiments in striated muscle fibres. *Journal of Physiology*. 208:607–644.
- Adrian, R. H., and C. L.-H. Huang. 1984*a*. Charge movements near the mechanical threshold in skeletal muscle of *Rana temporaria*. *Journal of Physiology*. 349:483–500.
- Adrian, R. H., and C. L.-H. Huang. 1984*b*. Experimental analysis of the relationship between charge movement components in skeletal muscle of *Rana temporaria*. *Journal of Physiology*. 353:419–434.

- Adrian, R. H., and A. Peres. 1979. Charge movement and membrane capacity in frog skeletal muscle. *Journal of Physiology*. 289:83–97.
- Adrian, R. H., and R. F. Rakowski. 1978. Reactivation of membrane charge movement and delayed potassium conductance in skeletal muscle fibres. *Journal of Physiology*. 278:533–557.
- Argiro V. 1981. Excitation-contraction uncoupling of striated muscle fibres by formamide treatment: evidence of detubulation. *Journal of Muscle Research and Cell Motility* 2:283–294.
- Buckingham, J. H., and L. A. Staehelin. 1969. The effect of glycerol on the structure of lecithin membranes; a study by freeze-etching and X-ray diffraction. *Journal of Microscopy*. 90:83–106.
- Chandler, W. K., R. F. Rakowski, and M. F. Schneider. 1976a. A non-linear voltage dependent charge movement in frog skeletal muscle. *Journal of Physiology*. 254:245–283.
- Chandler, W. K., R. F. Rakowski, and M. F. Schneider. 1976b. Effect of glycerol treatment and maintained depolarization on charge movement in skeletal muscle. *Journal of Physiology*. 254:285–316.
- Curtis, B. M., and W. A. Caterall. 1984. Purification of the calcium antagonist receptor of the voltage-sensitive calcium channel from skeletal muscle transverse tubules. *Biochemistry*. 23:2113–2118.
- Duane, S., and C. L.-H. Huang. 1982. A quantitative description of the voltage-dependent capacitance in frog skeletal muscle in terms of equilibrium statistical mechanics. *Proceedings of the Royal Society of London*. B215:75–94.
- Dulhunty, A. F., and C. Franzini-Armstrong. 1975. The relative contributions of the folds and caveolae to the surface membrane of frog skeletal muscle fibres at different sarcomere lengths. *Journal of Physiology*. 250:513–539.
- Dulhunty, A. F., and P. W. Gage. 1973. Differential effects of glycerol treatment on membrane capacity and excitation-contraction coupling in toad sartorius fibers. *Journal of Physiology*. 234:373–408.
- Eisenberg, R. S., J. N. Howell, and P. C. Vaughan. 1971. The maintenance of resting potentials in glycerol-treated muscle fibres. *Journal of Physiology*. 215:95–102.
- Eisenberg, B. R., and R. L. Milton. 1984. Muscle fiber termination at the tendon in the frog's sartorius: a stereological study. *American Journal of Anatomy*. 171:273–284.
- Franzini-Armstrong, C. 1975. Membrane particles and transmission at the triad. *Federation Proceedings*. 34:1382–1389.
- Fujino, M., T. Yamaguchi, and K. Suzuki. 1961. "Glycerol effect" and the mechanism linking excitation of the plasma membrane with contraction. *Nature*. 192:1159–1161.
- Gage, P. W., and R. S. Eisenberg. 1969a. Capacitance of the surface and transverse tubular membrane of frog sartorius muscle fibers. *Journal of General Physiology*. 53:265–278.
- Gage, P. W., and R. S. Eisenberg. 1969b. Action potentials, afterpotentials and excitation-contraction coupling in frog sartorius fibers without transverse tubules. *Journal of General Physiology*. 53:298–310.
- Hidalgo, C., M. A. Carrasco, K. Magendzo, and E. Jaimovich. 1986. Phosphorylation of phosphatidylinositol by transverse tubule vesicles and its possible role in excitation-contraction coupling. *FEBS Letters*. 202:69–73.
- Hodgkin, A. L., and S. Nakajima. 1972a. The effects of diameter on the electrical constants of frog skeletal muscle fibres. *Journal of Physiology*. 221:105–120.
- Hodgkin, A. L., and S. Nakajima. 1972b. Analysis of the membrane capacity in frog muscle. *Journal of Physiology*. 221:121–136.
- Horowicz, P., and M. F. Schneider. 1981. Membrane charge movement in contracting and non-contracting skeletal muscle fibres. *Journal of Physiology*. 314:565–593.
- Howell, J. A., and D. J. Jenden. 1967. T-tubules of skeletal muscle: morphological alterations which interrupt excitation-contraction coupling. *Federation Proceedings*. 26:553. (Abstr.)

- Huang, C. L.-H. 1980. Charge movement components in skeletal muscle. *Journal of Physiology*. 305:31–32P.
- Huang, C. L.-H. 1981a. Dielectric components of charge movements in skeletal muscle. *Journal of Physiology*. 313:187–205.
- Huang, C. L.-H. 1981b. Effects of local anaesthetics on the relationship between charge movements and contractile thresholds in frog skeletal muscle. *Journal of Physiology*. 320:381–391.
- Huang, C. L.-H. 1982. Pharmacological separation of charge movement components in frog skeletal muscle. *Journal of Physiology*. 324:375–387.
- Huang, C. L.-H. 1984. Analysis of “off” tails of intramembrane charge movements in skeletal muscle of *Rana temporaria*. *Journal of Physiology*. 356:375–390.
- Huang, C. L.-H. 1986. The differential effects of twitch potentiators on charge movements in frog skeletal muscle. *Journal of Physiology*. 380:17–33.
- Huang, C. L.-H. 1987. “Off” tails of intramembrane charge movements in frog skeletal muscle in perchlorate-containing solutions. *Journal of Physiology*. 384:491–510.
- Hui, C. S. 1983. Pharmacological studies of charge movements in frog skeletal muscle. *Journal of Physiology*. 337:509–552.
- Jaimovich, E., R. A. Venosa, P. Shrager, and P. Horowicz. 1976. Density and distribution of tetrodotoxin receptors in normal and detubulated frog sartorius muscle. *Journal of General Physiology*. 67:399–416.
- Krolenko, S. A. 1969. Changes in the T system of muscle fibres under the influx and efflux of glycerol. *Nature*. 221:966–968.
- Lamb, G. D. 1986. Components of charge movement in rabbit skeletal muscle: the effect of tetra-caine and nifedipine. *Journal of Physiology*. 376:85–100.
- Melzer, W., M. F. Schneider, B. J. Simon, and G. Szucs. 1986. Intramembrane charge movement and calcium release in frog skeletal muscle. *Journal of Physiology*. 373:481–512.
- Milton, R. L., R. T. Mathias, and R. S. Eisenberg. 1985. Electrical properties of the myotendon region of frog twitch muscle fibers measured in the frequency domain. *Biophysical Journal*. 48:253–267.
- Nakajima S., Y. Nakajima, and L. D. Peachey. 1973. Speed of repolarization and morphology of glycerol-treated frog muscle fibres. *Journal of Physiology*. 234:465–480.
- Peachey, L. D. 1965. The sarcoplasmic reticulum and transverse tubules of the frog's sartorius. *Journal of Cell Biology*. 25:209–231.
- Rakowski, R. F., P. M. Best, and M. R. James-Kracke. 1985. Voltage dependence of membrane charge movement and calcium release in frog skeletal muscle. *Journal of Muscle Research and Cell Motility*. 6:403–433.
- Rios, E., and G. Brum. 1987. Involvement of dihydropyridine receptors in excitation-contraction coupling in skeletal muscle. *Nature*. 325:717–720.
- Schneider, M. F., and W. K. Chandler. 1973. Voltage-dependent charge in skeletal muscle: a possible step in excitation-contraction coupling. *Nature*. 242:244–246.
- Schwartz, L. M., E. W. McClesky, and W. Almers. 1985. Dihydropyridine receptors in muscle are voltage-dependent but most are not functional calcium channels. *Nature*. 314:747–751.
- Vergara, J., R. Y. Tsien, and M. Delay. 1985. Inositol 1,4,5-triphosphate: a possible chemical link in excitation-contraction coupling in muscle. *Proceedings of the National Academy of Sciences*. 82:6352–6356.